Journal of Electronic Research and Application, 2026, Volume 10, Issue 2
http://ojs.bbwpublisher.com/index.php/JERA
ISSN Online: 2208-3510
ISSN Print: 2208-3502

Research on the Engineering Implementation of UAV Attitude Estimation Based on Multi-Sensor Fusion

Qi Li, Jianbo Zhou

Beijing Information Technology College, Beijing 100015, China

Abstract: Aiming at the practical problems such as insufficient accuracy and poor robustness when a single sensor is used for UAV attitude estimation, this paper proposes a multi-sensor fusion algorithm based on the Extended Kalman Filter (EKF). With the Inertial Measurement Unit (IMU) as the core sensing component, the scheme fuses Global Positioning System (GPS) and magnetometer data to construct a 16-dimensional state space model, realizing the joint solution of UAV attitude, velocity, and position information. Experimental verification shows that in static tests, the Root Mean Square Error (RMSE) of pitch and roll angle estimation errors is significantly reduced; in dynamic test scenarios, the attitude tracking accuracy is significantly improved compared with the traditional complementary filter algorithm. On this basis, this paper further builds a modular experimental platform for vocational education practice, decomposing the algorithm implementation process into four core teaching modules: sensor data collection, error calibration, state prediction, and measurement update. It provides reusable teaching cases and a complete engineering implementation idea for the curriculum reform of the UAV application technology major in higher vocational colleges.

Keywords: Multi-sensor fusion; Attitude estimation; Extended Kalman Filter (EKF); UAV system

Online publication: March 31, 2026

1. Theoretical basis of attitude estimation

1.1. Coordinate system definition and transformation relationship

A clear transformation logic between multiple coordinate systems is a core prerequisite for UAV attitude estimation, which guarantees the subsequent estimation accuracy [1]. This paper specifically defines the following two types of core coordinate systems.

1.1.1. Navigation coordinate system (n-frame)

This system adopts the North-East-Down (NED) coordinate system, with the origin fixed at the observation point on the Earth's surface, the X-axis pointing to geographic north, the Y-axis to geographic east, and the Z-axis

vertically downward toward the center of the Earth.

1.1.2. Body coordinate system (b-frame)

This system fixed to the UAV's center of gravity, the X-axis along the nose forward, the Y-axis to the right of the fuselage belly, and the Z-axis perpendicular to the X-Y plane toward the fuselage belly, forming a right-hand coordinate system [2].

The attitude matrix C_b^n describes the rotation transformation from the body coordinate system to the navigation coordinate system. Using quaternion $q = [q_0, q_1, q_2, q_3]^T$ to represent it can avoid the singularity problem of Euler angles. The corresponding relationship between the quaternion and the attitude matrix is:

$$C_b^n = \begin{bmatrix} q_0^2 + q_1^2 - q_2^2 - q_3^2 & 2(q_1q_2 - q_0q_3) & 2(q_1q_3 + q_0q_2) \\ 2(q_1q_2 + q_0q_3) & q_0^2 - q_1^2 + q_2^2 - q_3^2 & 2(q_2q_3 - q_0q_1) \\ 2(q_1q_3 - q_0q_2) & 2(q_2q_3 + q_0q_1) & q_0^2 - q_1^2 - q_2^2 + q_3^2 \end{bmatrix}$$

1.2. Sensor error model

1.2.1. IMU error model

The output of gyroscopes and accelerometers includes deterministic errors and random errors. Deterministic errors mainly include bias error b and scale factor error s , while random errors are mainly modeled as Gaussian white noise w and first-order Markov process m [3]. The gyroscope measurement model is:

$$w_m = w_{true} + b_g + S_g \cdot w_{true} + m_g + W_g$$

The accelerometer measurement model is:

$$a_m = a_{true} + b_a + S_a \cdot a_{true} + m_a + W_a$$

where subscripts g and a correspond to gyroscopes and accelerometers respectively, m denotes measured values, and true denotes true values.

1.2.2. GPS error model

The position and velocity information provided by GPS has delays and noise. The position measurement model is:

$$p_{GPS} = P_{true} + v_p$$

where v_p~N(0, R_{GPS}) is measurement noise, and the covariance matrix R_{GPS} is related to satellite geometric distribution (HDOP/VDOP).

1.2.3. Magnetometer error model

The magnetometer measures the local magnetic field vector, and its output model is:

$$m_m = C_b^n \cdot m_{earth} + b_m + v_m$$

where m_{earth} is the geomagnetic field vector in the navigation coordinate system, b_m is the bias caused by hard magnetic interference, and v_m is measurement noise.

2. Design of multi-sensor fusion algorithm

2.1. System architecture

The fusion system designed in this paper adopts a hierarchical architecture. The bottom layer is the sensor data collection layer, responsible for acquiring and preprocessing raw data; the middle layer is the filtering and calculation layer, performing state prediction and measurement update; the upper layer is the application interface layer, providing attitude, velocity, and position information to the flight control system [4–7].

2.2. Construction of state space model

A 16-dimensional state vector is selected:

$$x = \left[q_0, q_1, q_2, q_3, \omega_x, \omega_y, \omega_z, v_n, v_e, v_d, p_n, p_e, p_d, b_{gx}, b_{gy}, b_{gz}\right]^T$$

Among them, the first four dimensions are quaternions, dimensions 5-7 are body angular velocities, dimensions 8-10 are navigation frame velocities, dimensions 11-13 are positions, and the last three dimensions are gyroscope biases.

The state prediction equation is based on the IMU kinematic model:

$$\dot{q} = \frac{1}{2}\Omega\left(\omega_m - b_g - w_g\right) \cdot q$$

$$\dot{v} = C_b^n \cdot (a_m - b_a - w_a) + g^n$$

$$\dot{p} = v$$

$$\dot{b}_g = w_{bg}$$

where $\Omega(\cdot)$ is the quaternion multiplication matrix, and $g^n = [0,0,9.81]^T$ is the gravity vector.

After discretization, the state transition equation is obtained:

$$x_{k|k-1} = f(x_{k-1}, u_k) + w_k$$

The process noise covariance matrix Qk is determined according to the IMU Allan variance analysis results, and the diagonal elements correspond to the prediction uncertainty of each state quantity.

2.3. Design of measurement model

Two types of measurement updates are designed.

2.3.1. GPS measurement update

GPS provides position and velocity measurements, and the measurement equation is:

$$z_{GPS} = \begin{bmatrix} p_n \\ p_e \\ p_d \\ v_n \\ v_e \\ v_d \end{bmatrix}_k + v_{GPS}$$

The measurement matrix HGPSH extracts the corresponding position and velocity components from the state vector:

$$H_{GPS} = [0_{6\times4}0_{6\times3}I_{3\times3}0_{3\times3}I_{3\times3}0_{3\times3}0_{6\times3}]$$

2.3.2. Magnetometer measurement update

Magnetometer measurements are used to correct heading angle drift. By converting the geomagnetic field vector in the navigation frame to the body frame and compare it with the magnetometer measurement value:

$$z_{mag} = m_m - C_n^b(q) \cdot m_{earth}$$

The Jacobian matrix of the measurement equation with respect to the quaternion is calculated to obtain H_{mag}, realizing heading angle error correction.

2.4. Adaptive covariance adjustment mechanism

Traditional EKF uses a fixed measurement noise covariance matrix, which is difficult to adapt to changes in dynamic environments. This paper designs an adaptive adjustment strategy:

For GPS measurements, dynamically modify the covariance according to the Horizontal Dilution of Precision (HDOP) and Vertical Dilution of Precision (VDOP):

$$R_{GPS} = R_{GPS0} \cdot (1 + \alpha \cdot HDOP^2 + \beta \cdot VDOP^2)$$

For magnetometers, identify interference by detecting the magnitude deviation of the magnetic field strength:

$$\Delta H = |m_m| - |m_{earth}|$$

When $\Delta H > \gamma$, increase the magnetometer measurement noise covariance:

$$R_{mag} = R_{mag0} \cdot (1 + k \cdot \Delta H^2)$$

This mechanism effectively reduces the impact of abnormal measurement values on the filter.

3. Design and implementation of experimental platform

3.1. Software architecture design

The software system is built based on the FreeRTOS real-time operating system, divided into four task threads, as shown in **Figure 1**.

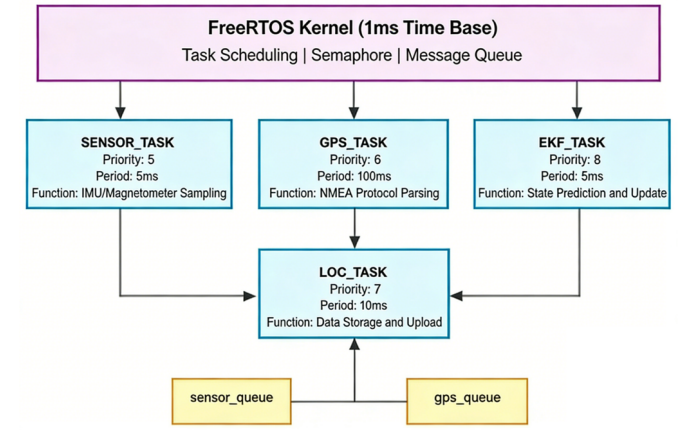

Figure 1. Software task scheduling architecture based on FreeRTOS.

3.2. Teaching modular design

To facilitate higher vocational students' understanding and implementation, the algorithm is decomposed into four teaching modules.

3.2.1. Module 1: Sensor data collection and calibration

Students read ICM-20602 raw data through the I²C protocol and learn the Allan variance analysis method to calibrate bias and noise parameters. A six-position calibration experiment is designed to calculate the installation error matrices of accelerometers and magnetometers [8–11].

3.2.2. Module 2: Quaternion kinematics implementation

Implement numerical integration of the quaternion differential equation, and compare the precision differences between the first-order Runge-Kutta method and the fourth-order Runge-Kutta method. Verify the impact of different integration step sizes on attitude calculation errors through MATLAB simulation.

3.2.3. Module 3: EKF algorithm programming

Implement matrix operation subroutines based on the STM32 standard peripheral library. Focus on explaining the maintenance of covariance matrix symmetry and positive definiteness check to avoid numerical calculation divergence. Provide unit test cases to verify the correctness of prediction and update steps.

3.2.4. Module 4: Experimental design for fusion strategy optimization

Add a GPS signal quality indicator light for students to intuitively observe the influence of HDOP (Horizontal Dilution of Precision) changes on the filter convergence speed. Design a magnetic field interference simulation experiment: use permanent magnets to gradually approach the magnetometer to construct an interference environment, thereby observing the actual effect of the adaptive covariance adjustment mechanism [12,13].

4. Teaching application and practice

4.1. Curriculum system integration

Integrate the multi-sensor fusion algorithm into the course "UAV Flight and Aerial Photography", setting 32 class hours of theoretical teaching and 16 class hours of experimental teaching. The theoretical part focuses on explaining state space model construction, Kalman filter derivation, and multi-sensor spatiotemporal registration [14,15]. Based on the platform described in this paper, students complete the following task chain in groups in the experimental part.

4.1.1. Task 1: Sensor data collection program design (4 class hours)

Implement the I^2C driver, read IMU raw data, and observe the original waveform through serial port printing.

4.1.2. Task 2: Sensor error calibration experiment (4 class hours)

Use a precision three-axis turntable for six-position calibration, calculate the bias, scale factor error, and installation error matrix, and analyze the improvement effect of attitude calculation accuracy before and after calibration.

4.1.3. Task 3: EKF algorithm programming implementation (6 class hours)

Implement matrix operations based on the CMSIS-DSP library, complete the coding of prediction and update steps, and verify the algorithm correctness through simulation data.

4.1.4. Task 4: Fusion strategy parameter tuning (2 class hours)

Adjust the process noise and measurement noise covariance matrices, observe the influence of different parameters on the filter convergence speed and steady-state accuracy, and write a parameter tuning experiment report.

4.2. Evaluation of teaching effect

To verify the teaching effectiveness, a comparative teaching experiment was conducted on two parallel classes of the 2023 UAV course. The experimental class adopted the modular platform teaching described in this paper, while the control class used the traditional theoretical teaching mode. Learning effectiveness was evaluated through final project assessment and questionnaire surveys. The project assessment requires students to independently complete the construction and debugging of the UAV attitude estimation system. The scoring dimensions include function implementation (40%), precision indicators (30%), code standardization (20%), and document completeness (10%).

5. Conclusion

Focusing on the core problems of accuracy and robustness in UAV attitude estimation, this paper proposes a multi-sensor fusion algorithm framework based on EKF and builds a modular experimental platform for higher vocational education. The main conclusions are as follows. Future research can proceed in the following directions:

(1) Explore nonlinear estimation schemes based on Unscented Kalman Filter or Particle Filter to further improve the estimation accuracy of the system under high maneuvering conditions;

(2) Conduct research on multi-UAV collaborative attitude estimation, and improve the system redundancy performance with the help of relative measurement information;

(3) Build a virtual simulation experimental platform, realize algorithm pre-verification relying on digital twin technology, and reduce the safety risks and costs of real-machine experiments;

(4) Promote the connection with the vocational skill certificate system, accurately align the core skill points of the platform with the UAV assembly and commissioning vocational skill level standards, and help improve students' employment competitiveness.

Disclosure statement

The author declares no conflict of interest.

References

[1] Li X, Zhang Q, Liu X, et al., 2025, A Multi-Moving Target Recognition Method Under UAV Platform Based on Deep Learning. Journal of Air Force Engineering University, 26(6): 85–95.

[2] Shen W, Zhong L, 2025, Review of UAV Inspection Optimization Modeling Methods. Journal of South China University of Technology (Natural Science Edition), 1–8.

[3] Wang X, Qi G, Li Y, et al. 2025, Research on Self-Calibration Algorithm of UAV Micro-Inertial Sensor. Space Electronic Technology, 1–7.

[4] Ma J, Fan L, Yao L, et al., 2025, Occlusion-Resistant Target Tracking Algorithm Based on Scale Feature Pyramid and Adaptive Kalman Filter. Journal of Taiyuan University of Technology, 1–15.

[5] Zhang B, Wang J, Sun H, et al., 2025, A Cross-Media UAV Water Entry and Exit Switching Control for Tandem Dual-Rotor. Control and Decision, 1–14.

[6] Yang J, Li Y, 2025, Research on Dynamic Object Tracking for Robot Visual Servo Based on Kalman Filter. Metrology & Measurement Technology, 51(11): 80–84.

[7] Yin Q, Ding J, Nie Z, 2025, YOLO-AirPose: Human Pose Estimation Algorithm from UAV Aerial Photography Perspective. Journal of Computer Applications, 1–10.

[8] Liu E, Li H, Ji S, et al., 2025, Research on the Application of Multi-Rotor UAV in Intelligent Inspection of Power Distribution Networks. Automation & Instrumentation, 2025(9): 117–122.

[9] Ye M, Dai Y, Lü F, 2025, UAV Hook Tip Operation Target Prediction Based on Dual Kalman Filter. Southern Agricultural Machinery, 56(5): 30–33.

[10] Wang D, Zhu C, Ji X, et al., 2025, UAV Attitude Estimation Based on Quaternion SRCKF-SLAM Algorithm. Journal of Xinyang Normal University (Natural Science Edition), 38(4): 428–436.

[11] Shang Y, Su J, Wei S, et al., 2024, An Improved Master-Slave UAV Collaborative Navigation Algorithm. Journal of Nanjing University of Aeronautics and Astronautics, 56(6): 1097–1103.

[12] Li D, Zhong M, 2024, UAV Attitude Estimation Method Based on Multi-Scale Feature Fusion. Enterprise Science and Technology & Development, 2024(11): 94–98.

[13] Zhang Z, Yang Y, 2025, Research on Sensor Bias Fault of Quadrotor UAV Based on Adaptive Sliding Mode Control. Journal of Sensor Technology and Application, 2025, 13.

[14] Ai J, Zhang X, Zheng L, et al., 2025, End Position and Joint Attitude Estimation Method of Aerial Work Manipulator Based on SLAM. Instrument Technique and Sensor, 2025(2): 122–126.

[15] Ye Y, Shi S, Lan T, et al., 2025, Real-Time Human Pose Estimation Network Based on Attention Refinement. Transducer and Microsystem Technologies, 44(2): 104–107.